

Role of Intramolecular Hydrogen Bonds in the Intermolecular Hydrogen Bonding of Carbohydrates

F. Javier Luque* and José María López

Departament de Fisicoquímica, Facultat de Farmàcia, Universitat de Barcelona, Avda Diagonal s/n, Barcelona 08028, Spain

Manuela López de la Paz and Cristina Vicent

Departamento de Química Orgánica Biológica, Instituto de Química Orgánica, CSIC, Juan de la Cierva 3, Madrid 28006, Spain

Modesto Orozco*

Departament de Bioquímica i Biologia Molecular, Facultat de Química, Universitat de Barcelona, Martí i Franquès 1, Barcelona 08028, Spain

Received: March 31, 1998

The cooperativity effects in hydrogen-bonded intermolecular interactions of carbohydrates are examined in this study. The nature of such effects is explored with ab initio quantum mechanical and density functional methods. Calculations are performed for complexes of 1,3-propanediol and *n*-propanol, which are used as model compounds to analyze hydrogen bond cooperativity in the dimerization of the sugar 1,3-diaxial diol 1,6-anhydro-3-deoxy-3-*N*-methylamine- β -D-glucopyranose. In addition to the influence of cooperativity in the binding energy, the magnitude of cooperativity effects is also examined from the change in key properties related to the formation of hydrogen bonds between monomers, which include bond lengths, atomic partial charges, electron density at bond critical points, and stretching frequencies. The results reported here provide a basis to discuss the relevance of cooperativity in molecular recognition of carbohydrates.

Introduction

Molecular recognition of carbohydrates is largely determined by the content of polar hydroxyl groups and their relative location in the carbohydrate.^{1–5} The formation of intramolecular hydroxyl–hydroxyl hydrogen bonds and other noncovalent interactions determines a variety of processes, such as crystallization, the assembly of carbohydrates in supramolecular structures, and the binding of carbohydrates by proteins in biological events, like cell–cell recognition, immune response, and blood coagulation. Therefore, knowledge of the energetics of OH...OH hydrogen bonding in carbohydrates is of fundamental interest to understand these properties in sugars.

A relevant feature of multiply hydrogen-bonded complexes is the nonadditivity of intermolecular interactions, which has given rise to the concept of cooperativity. Since the early studies,⁶ a great research effort has been focused on the characterization and quantitative evaluation of cooperativity in a variety of hydrogen-bonded networks. Much interest is paid to water oligomers, since cooperativity is believed to be important for the structure and properties of water in its states of aggregation.⁷ Cooperativity has also been examined in other molecular systems, like protonated hydrates,⁸ hydrogen halides,⁹ hydrogen cyanide,¹⁰ hydrogen peroxide,¹¹ or alcohols.¹² Of particular relevance owing to its biological implications is the nonadditivity in amide hydrogen bonds¹³ since they can be relevant to understand the structure and stability of peptides and proteins and the role of solvents on such properties.

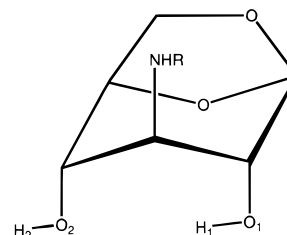


Figure 1. Structure of the [2,4 (*a,a*) *cis*] diol derivative of 1,6-anhydro- β -D-glucopyranose used in self-assembly studies in chloroform. (R = $-\text{CO}-(\text{CH}_2)_{14}-\text{CH}_3$ in ref 16).

The size of glycosidic units, the existence of multiple H-bonding patterns, and the lability of hydrogen bonds make difficult the study of nonadditive effects in carbohydrates. In addition to the nature of donor/acceptor groups, the network of hydrogen bonds is highly sensitive to the arrangement and stereochemistry of hydroxyl groups and the surrounding medium. This makes it necessary to resort to experimental techniques like neutron diffraction data of crystalline structures and spectroscopic techniques in solution to assess the role of cooperativity in molecular recognition.¹⁴ In this context theoretical methods¹⁵ can also provide insight into the physical basis of nonadditivity of hydrogen bonding in carbohydrates.

The effect of intramolecular hydrogen bonds on the assembly of 1,6-anhydro-3-deoxy-3-hexadecamide- β -D-glucopyranose has been recently studied using experimental techniques.¹⁶ It was found that the 1,3-diaxial diol species (Figure 1) self-assembled in chloroform solution at 299 K with a dimerization constant of 70 M^{-1} and that the assembly was mediated by intermolecular

* To whom correspondence should be addressed.

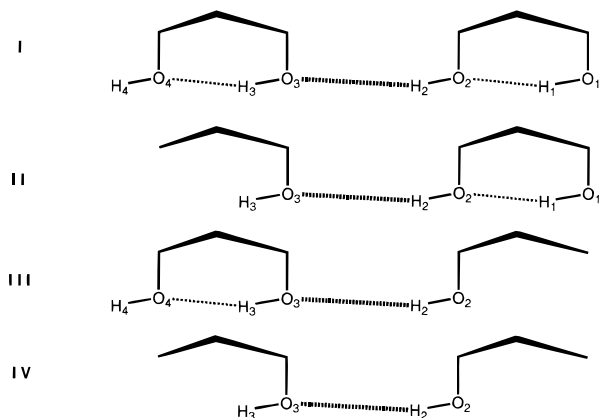


Figure 2. Schematic representation of the four bimolecular complexes formed with 1,3-propanediol and *n*-propanol.

hydrogen bonding between hydroxyl groups. However, no dimerization was observed for the monoalcohol species. This led to the conclusion that the addition of one extra hydroxyl group in a pyranoid ring having a 1,3-*syn* diaxial orientation accounted for an extra stabilization of the dimer, compared to the monoalcohols. These findings suggested the existence of strong intermolecular cooperativity due to the intramolecular 1,3-hydrogen bond, whose directionality was determined to be O(1)H → O(2)H (see Figure 1).

The aim of this study is to analyze in detail the hydrogen bond cooperativity in the assembly of the 1,3-diaxial diol derivative. Calculations are performed to examine the influence of intramolecular hydrogen bonding on the dimerization energy. In addition, attention is also paid to the changes in structural parameters, like O...O distances and O–H bond lengths and the donor O–H harmonic vibrational frequencies. Finally, discussion of the cooperativity effect is made from the changes in atomic partial charges and in the topological characteristics of the electronic charge distribution in OH...OH hydrogen bonds.

Methods

Ab initio quantum mechanical and density functional calculations were performed to examine the role of intramolecular hydrogen bonding on the dimerization of the glucopyranose derivative (Figure 1). An accurate description of hydrogen bonding requires very flexible basis sets, which makes advisable the use of reduced models. Thus, 1,3-propanediol and *n*-propanol were used as model compounds of the di- and monohydroxylated forms of the pyranose ring. The bimolecular complexes of 1,3-propanediol and *n*-propanol, as well as the dimers formed by mixing those compounds, were considered in calculations (Figure 2). The molecular geometries were optimized at the HF/6-31G(d)¹⁷ level. The minimum-energy nature of optimized structures was verified from analysis of the vibrational frequencies. The binding energies were determined at the SCF level with the 6-31G(d) and 6-311++G(d,p)¹⁸ basis, and the effect of electron correlation was examined by means of MP2¹⁹ and B3LYP²⁰ calculations using the 6-311++G(d,p) basis. In all cases the basis-set superposition error was corrected using the counterpoise method.²¹ The zero-point energy correction was estimated from the HF vibrational frequencies scaled by 0.893.²² Finally, the influence of functional groups of the pyranose ring on the binding energy was examined. Full geometry optimizations at the HF/6-31G(d) levels were performed for the dimer formed by two pyranose rings (R: H; Figure 1), and the minimum-energy nature of the stationary point was also verified from frequency analysis.

In addition to the binding energies, the contribution of different energy components was examined from the generalized molecular interaction potential with polarization (GMIPp; eq 1), which provides the interaction energy between a quantum mechanical molecule with a set of classical particles.²³ The interaction energy is expressed as the addition of three terms: electrostatic, polarization, and van der Waals terms. The electrostatic energy is determined from the electrostatic potential²⁴ computed rigorously at the position of every classical particle, each having a net charge Q_n . The polarization energy is computed using a generalized procedure of the perturbative approach proposed by Francl,²⁵ and the van der Waals energy is determined using a classical 12-6 formalism. Calculations were performed using wave functions determined at the HF/6-31G(d) level for the isolated monomers. Atomic charges were derived by fitting to the HF/6-31G(d) electrostatic potential of the dimer²⁶ imposing electric neutrality of the monomers. The van der Waals parameters for the quantum molecule were taken from our previous parameterization of the molecular solvation potential (ref 27; $\epsilon(\text{C})$, 0.0013; $\epsilon(\text{O})$, 0; 0.121; $\epsilon(\text{H})$; 0. kcal/mol; $r(\text{C}) = 3.263$, $r(\text{O}) = 2.319$, $r(\text{H}) = 0$. Å), whereas those of the classical molecule were taken from the OPLS forcefield (ref 15b; $\epsilon(\text{C})$; 0.066; $\epsilon(\text{O})$, 0.170; $\epsilon(\text{H bound to C})$, 0.030; $\epsilon(\text{H bound to O})$, 0. kcal/mol; $r(\text{C}) = 1.964$, $r(\text{O}) = 1.751$, $r(\text{H bound to C}) = 1.403$, $r(\text{H bound to O}) = 1.403$ 0. Å).

$$\text{GMIPp} = E_{\text{ele}} + E_{\text{pol}} + E_{\text{vw}} \quad (1)$$

$$E_{\text{ele}} = \sum_{m=1}^M \sum_{n=1}^N \frac{Z_m Q_n}{|\mathbf{R}_m - \mathbf{R}_n|} - \sum_{\mu} \sum_{\nu} \sum_{n=1}^N P_{\mu\nu} \int \chi_{\mu}(\mathbf{r}) \frac{Q_n}{|\mathbf{r} - \mathbf{R}_n|} \chi_{\nu}(\mathbf{r}) \, \text{dr} \quad (1a)$$

$$E_{\text{pol}} = \sum_{i=1}^{\text{occ}} \sum_{j=1}^{\text{vir}} (\xi_i - \xi_j)^{-1} \times \left\{ \sum_{\mu \in i} \sum_{\nu \in j} c_{\mu i} c_{\nu j} \int \chi_{\mu}(\mathbf{r}) \sum_{n=1}^N \frac{Q_n}{|\mathbf{r} - \mathbf{R}_n|} \chi_{\nu}(\mathbf{r}) \, \text{dr} \right\}^2 \quad (1b)$$

$$E_{\text{vw}} = \sum_{m=1}^M \sum_{n=1}^N \epsilon_{mn} \left\{ \left(\frac{R_{mn}^*}{|\mathbf{R}_m - \mathbf{R}_n|} \right)^{12} - 2 \left(\frac{R_{mn}^*}{|\mathbf{R}_m - \mathbf{R}_n|} \right)^6 \right\} \quad (1c)$$

where $R_{mn}^* = r_m + r_n$ and $\epsilon_{mn} = (\epsilon_m \epsilon_n)^{1/2}$.

The cooperativity effect was also examined from the changes in the intermolecular hydrogen bond O...O distance, the elongation of O–H bonds, and the shifts of the donor O–H stretching frequencies. Moreover, changes in atomic partial charges of hydroxyl groups were also examined. Furthermore, the topological properties of the hydrogen bond bond critical point were determined using Bader's theory of atoms in molecules.²⁸

Calculations were carried out with Gaussian-94.²⁹ The electron density analysis was performed with the program AIMPAC.³⁰ The GMIPp was computed using MOPETE/MOPFIT.³¹ Computations were carried out on the IBM-SP2 computer of the Centre de Supercomputació de Catalunya and on workstations in our laboratory.

Results and Discussion

The dimerization energies computed at the HF, MP2, and B3LYP levels for the complexes I–IV (see Figure 2) are given in Table 1. The geometries of the complexes were fully

TABLE 1: Binding Energies^a (kcal/mol) of the Complexes I–IV Computed at the HF, MP2, and B3LYP Levels of Theory

complex	HF ^b	HF ^c	MP2 ^c	B3LYP ^c	$\Delta(\text{ZPE})$	ΔE_{dist}
I ^d	-6.7 (-6.2) ^d	-6.2 (-5.8)	-7.5 (-7.2)	-7.1 (-6.7)	1.3	0.2
II	-5.5	-5.1	-6.5	-5.9	1.3	0.1
III	-5.1	-4.7	-6.1	-5.6	1.2	0.1
IV	-4.4	-4.0	-5.4	-4.8	1.2	0.1

^a The calculations were performed using the geometries optimized at the HF/6-31G(d) level. The dimerization energies were corrected for the basis-set superposition error. The zero-point energy correction, $\Delta(\text{ZPE})$, and the energy change due to geometry distortion in the monomers, ΔE_{dist} , upon dimerization were determined at the HF/6-31G(d) level. ^b 6-31G(d) basis. ^c 6-311++G(d,p) basis. ^d The value in parentheses gives the binding energy estimated by assuming additivity of the enhancing effects on the dimerization energy due to formation of intramolecular hydrogen bonds in complexes II and III.

optimized at the HF/6-31G(d) level. The relative orientation of the two interacting units was similar in all cases and reflected the arrangement of the hydroxyl groups in the fully optimized geometry of the whole pyranose ring (Figure 3; see below). There is little difference in the dimerization energies computed at the HF level with the 6-31G(d) and 6-311++G(d,p) basis. Nevertheless, the inclusion of electron correlation at both MP2 and B3LYP levels leads to more favorable binding energies, which are around 1.3 and 0.9 kcal/mol larger (in absolute values) than the HF results. Similar findings have been reported for related hydrogen-bonded complexes.^{12b,32} Despite the differences between the binding energies determined from HF, MP2, and B3LYP calculations, there is complete agreement between all the methods about the influence of the cooperativity effect on the interaction between monomers on going from complex IV to complex I.

The results in Table 1 clearly show the strengthening of the intermolecular hydrogen bond arising upon formation of intramolecular hydrogen bonds. Thus, the binding energy for the dimer of 1,3-propanediol (complex I) is around 2.3 kcal/mol larger compared to the value for the dimer of *n*-propanol (complex IV). The formation of an intramolecular hydrogen bond on either of the two monomers (complexes II and III) leads to slightly different enhancements of the binding energy. Thus, addition of an hydroxyl group acting as a proton acceptor to the central hydrogen bond (complex III) increases the binding energy by 0.7 kcal/mol, whereas such an effect amounts to 1.1 kcal/mol when the hydroxyl group acts as proton donor to the intermolecular hydrogen bond (complex II). This effect can be attributed to the different arrangement of the hydrogen-bonded hydroxyl groups, which is nearly linear in complex II (angle O1–O2–O3 $\sim 155^\circ$), whereas the oxygen atoms deviate sensibly from linearity in complex III (angle O1–O2–O3 $\sim 110^\circ$).

Another interesting finding is the mutual cooperativity of the two hydroxyl groups vicinal to the central hydrogen bond. If their influence on the dimerization is assumed to be additive, the binding energy of complex I might be estimated by adding the stabilizing effect due to intramolecular hydrogen bonding in complexes II and III, which amounts to 1.8 kcal/mol, to the binding energy of complex IV. The results show that the binding energy of complex I is 0.5 kcal/mol more favorable than the value determined assuming additivity of the effects due to intramolecular hydrogen bonds. This contribution is far from being negligible since it accounts for around 20% of the total enhancement in the binding energy of complex I, compared to complex IV.

TABLE 2: Relative and Absolute (in Parentheses) Values of Electrostatic, Polarization, and van der Waals Energy Contributions (kcal/mol) to the Binding Energy of Complexes I–IV Determined from GMIPp Calculations^a

complex	E_{ele}	E_{pol}	E_{vw}	ΔE_{GMIPp}	$\Delta E_{\text{theor}}^b$
I	-3.0 (-9.5)	-0.3 (-0.6)	0.6 (3.0)	-2.7 (-7.1)	-2.3
II	-1.3 (-7.8)	-0.2 (-0.5)	0.3 (2.7)	-1.2 (-5.6)	-1.1
III	-1.2 (-7.7)	-0.1 (-0.4)	0.7 (3.1)	-0.6 (-5.0)	-0.7
IV	0.0 (-6.5)	0.0 (-0.3)	0.0 (2.4)	0.0 (-4.4)	0.0

^a Calculations performed by using wave functions and electrostatic-potential derived charges determined at the H F/6-31G(d) level and van der Waals parameters previously reported for the molecular solvation potential²⁷ and from OPLS force-field.^{15b} See text for more details. ^b Relative binding energies determined from values in Table 1.

Table 1 also reports the change in zero-point energy correction and the energy cost due to geometry distortion upon complexation. Since these energy terms are very similar in all the cases, they do not affect the relative binding energies of complexes I–IV. Moreover, the entropic contribution is expected to be similar for the dimerization of the different complexes. On this grounds, the results in Table 1 indicate that the enhanced binding of complex I compared to complex IV is enthalpically favored by the strong cooperativity between intra- and intermolecular hydrogen bonds. This effect, which amounts to around -2.3 kcal/mol, is in reasonable agreement with the available experimental data. Thus, whereas no dimerization was observed for the monohydroxylated derivatives of the pyranose ring,^{16b} the self-assembly of the diol derivatives was favored by -2.5 kcal/mol in chloroform solution and -3 kcal/mol in a chloroform/carbon tetrachloride mixture.^{16b}

In order to examine the origin of the hydrogen bond cooperativity, the contribution of electrostatic, polarization, and van der Waals energy components was determined from GMIPp calculations. The GMIPp values (see Table 2) are close to the interaction energies reported in Table 1. It is clear that the most important component of the binding energy is electrostatics and that this term alone explains the differences between the binding energies of complexes I–IV. This finding is not unexpected since electrostatics is known to modulate decisively the strength of hydrogen bonding. Indeed, it suggests that the relative arrangement between hydrogen bond donor and acceptor largely determines the magnitude of cooperative effects in multiply hydrogen-bonded complexes.

Table 3 gives the O \cdots O and O–H distances of the intra- and intermolecular hydrogen bonds. The stabilizing effect of the terminal hydroxyl groups on the central hydrogen bond is reflected in the decrease of the distance O2 \cdots O3, which diminishes around 0.08 Å from complex IV to complex I. On going from either complex II or III to complex I, such distance decreases by near 0.03 Å, this change being sensibly larger than the variations in the O \cdots O distances corresponding to the intramolecular hydrogen bonds (around 0.005 Å). It is also worth noting the enlargement of the bonds O2–H2 and O3–H3, which increase by 0.003 Å from complex IV to complex I, this effect being much larger than the variation, if observed, for the terminal O–H bonds.

The structural changes noted above are consistent with the variations in atomic partial charges determined from Mulliken population analysis,³³ which are given in Table 4. The charges on the oxygen atoms involved in the central hydrogen bond become more negative by 0.03 units of electron in complex I compared to the values in complex IV. This effect is by far more important than the changes observed in the partial charges of the oxygen atoms in the terminal hydroxyl groups. Indeed,

TABLE 3: O...O and O-H Distances (Å) of the Hydroxyl Groups Involved in Intra- and Intermolecular Hydrogen Bonds

complex	$d(\text{O1}-\text{H1})^a$	$d(\text{O1}\cdots\text{O2})$	$d(\text{O2}-\text{H2})$	$d(\text{O2}\cdots\text{O3})$	$d(\text{O3}-\text{H3})$	$d(\text{O3}\cdots\text{O4})$	$d(\text{O4}-\text{H4})$
I	0.9500	2.8032	0.9541	2.8624	0.9508	2.7852	0.9469
II	0.9497	2.8079	0.9527	2.8986	0.9470		
III			0.9522	2.9000	0.9505	2.7925	0.9469
IV			0.9511	2.9403	0.9470		

^a See Figure 2 for nomenclature. Values taken from the HF/6-31G(d) optimized geometries.

TABLE 4: Mulliken Partial Charges (Units of Electron) on the Oxygen and Hydrogen Atoms Involved in Intra- and Intermolecular Hydrogen Bonds

complex	O1 ^a	H1	O2	H2	O3	H3	O4	H4
I	-0.771	0.478	-0.821	0.514	-0.792	0.490	-0.765	0.453
II	-0.770	0.477	-0.816	0.508	-0.767	0.454		
III			-0.798	0.500	-0.786	0.487	-0.764	0.451
IV			-0.792	0.494	-0.762	0.452		

^a See Figure 2 for nomenclature. Values determined at the HF/6-31G(d) level.

TABLE 5: Topological Electron Density Properties of the Bond Critical Points in the Intermolecular Hydrogen Bond^a

complex	$\rho(\text{H2}\cdots\text{O3})^b$	$\nabla^2\rho^c$	λ_1^d	λ_2	λ_3	$\rho(\text{O2}-\text{H2})$	$\rho(\text{O3}-\text{H3})$
I	0.0276	0.0933	-0.0411	-0.0392	0.1736	0.3540	0.3599
II	0.0255	0.0862	-0.0372	-0.0354	0.1588	0.3562	0.3676
III	0.0251	0.0845	-0.0362	-0.0348	0.1550	0.3582	0.3608
IV	0.0232	0.0783	-0.0329	-0.0314	0.1427	0.3601	0.3681

^a All values in atomic units. ^b Electron density. ^c Laplacian of the electron density. ^d Eigenvalues of the Hessian of electron density.

the positive charge in the hydrogen atoms bound to O2 and O3 is enlarged by at least 0.02 units of electron, while the variation observed for the terminal hydroxyl groups is sensibly lower or even negligible. As a result, in complex I the polarity of the central hydroxyl (O2-H2, O3-H3) groups is sensibly larger than that of the terminal hydroxyl (O1-H1, O4-H4) groups. These effects are observed at all the levels of calculation used in this work.

The consistency of the preceding results can also be extended to the changes in electron density at the bond critical points. At this point, different studies have pointed out that formation of hydrogen bonds is associated to the appearance of a bond critical point between the hydrogen atom and the acceptor atom, which are linked by the concomitant bond path.³⁴ The topological analysis was performed using the HF/6-31G(d) wave functions. It must be noted that correlation effects have little influence on the number and nature of critical points found for this type of systems.³⁵

In all the complexes the intermolecular hydrogen bond was characterized by the presence of bond critical point between the hydrogen atom (H2) and the acceptor oxygen (O3) atom. It has been observed that for hydrogen bonds interactions the electron density, ρ , at the bond critical point is low and its curvature (determined from the Laplacian of the electron density, $\nabla^2\rho$) is positive, since these interactions are dominated by the contraction of charge away from the interatomic surface toward each nuclei.³⁴ These conditions are fulfilled in the bond critical points for the complexes I-VI (see Table 5). The electron density at the bond critical point ranges from 0.023 to 0.028 (in atomic units), which compares with the values reported for different hydrogen-bonded complexes, where the electron density was found to vary from 0.002 to 0.034 au.³⁴ Likewise, the range of values for the Laplacian of the electron density (0.078-0.093 au) also compares with previous results, which vary from 0.024 to 0.139 au.³⁴

The results in Table 4 shows that the charge density at the bond critical point of the intermolecular hydrogen bond increases by near 0.005 au on going from complex IV to complex I. Since there is a linear relationship between the interaction energy in

hydrogen-bonded complexes and the charge density at the bond critical point,³⁴ such an increase indicates a strengthening of the interaction O2-H2...O3, as noted in the results reported in Table 1. There is also a slight depletion of electron density at the bond critical point of bonds O2-H2 and O3-H3 (see Table 5). These changes indicate that the formation of intramolecular hydrogen bonds in complex I promotes an electron shift to the intermolecular hydrogen bond, which occurs mainly in the direction of the bond path, as noted by the fact that the largest variation of the three eigenvalues (λ_i , $i = 1, 3$) of the Hessian of electron density between complexes I and IV is found for the positive eigenvalue λ_3 . This electron charge redistribution is in agreement with the changes in atomic charges (Table 4), which indicated an increase of the positive (negative) charge in the hydrogen (oxygen) atoms of the hydroxyl groups joining the two monomers. In turn, the loss of electron density at the O-H bonds and increase of electron density in the hydrogen bond critical points agrees with the elongation of the O2-H2 and O3-H3 bonds and the shortening of the O2...O3 distance (Table 3).

In addition to the topological properties in Table 5, a set of atomic integrated properties have been recently considered to be indicative of hydrogen bonding.^{34d} They are referred to the hydrogen atom in the hydrogen bond and are determined by integration of the given quantity over the atomic basin. Such properties are the atomic charge (N), the energy of the atom (E), the dipolar polarization (M), and the atomic volume (V). Table 6 gives the corresponding values for the hydrogen atoms of the hydroxyl groups involved in the intermolecular hydrogen bond (H2 and H3) in complexes I-IV. The results show that, on going from complex IV to complex I, the net positive charge on the hydrogen atom is enhanced and the atomic volume decreases, as expected from the electron shift mentioned above, leading to a decrease of the atomic first moment and to a destabilization of the hydrogen atom. These trends reflect the strengthening of the intermolecular hydrogen bonding arising from cooperativity with intramolecular hydrogen bonds.

Further insight into the cooperativity of intramolecular hydrogen bonds on intermolecular hydrogen bonding is afforded

TABLE 6: Atomic Properties (atomic units) Integrated for the Hydrogen Atoms in the Intermolecular Hydrogen Bond

complex	bond	N^a	E^b	M^c	V^d
I	O2-H2	0.648	-0.3203	0.127	12.1
	O3-H3	0.636	-0.3284	0.186	14.1
II	O2-H2	0.642	-0.3237	0.262	12.7
	O3-H3	0.597	-0.3517	0.305	19.3
III	O2-H2	0.635	-0.3292	0.333	12.9
	O3-H3	0.634	-0.3306	0.361	14.2
IV	O2-H2	0.631	-0.3322	0.385	13.5
	O3-H3	0.594	-0.3534	0.417	19.5

^a Net charge. ^b Energy of the atom. ^c Dipolar polarization. ^d Atomic volume corresponding to an isodensity surface of 0.001 au.

TABLE 7: Harmonic Stretching Frequencies (cm^{-1}) of the O-H Bonds Involved in Intra- and Intermolecular Hydrogen Bonds

complex	$\nu(\text{O1-H1})$	$\nu(\text{O2-H2})$	$\nu(\text{O3-H3})$	$\nu(\text{O4-H4})$
I	3636	3563	3632	3677
II	3641	3588	3677	
III		3592	3635	3677
IV		3613	3677	

by inspection of the O-H harmonic frequencies, which has been used to quantitate the magnitude of cooperative effects in hydrogen-bonded complexes.³⁶ The O-H stretching frequencies determined for complexes I-IV are given in Table 7. The lowest and largest frequencies in complex I correspond to the bonds O2-H2 and O4-H4, respectively. Let us note that the group involved in intermolecular hydrogen bonding (O2-H2) is that having the largest bond length (Table 3) and ionic character (Table 4), whereas the free terminal group (O4-H4) has the lowest bond length and charge separation. Indeed, the ordering of vibrational frequencies (O2-H2 < O3-H3 ~ O1-H1 < O4-H4) reflects the variation of electron density at the corresponding bond critical points (O1-H1, 0.3625; O2-H2, 0.3540; O3-H3, 0.3599; O4-H4, 0.3667 au).

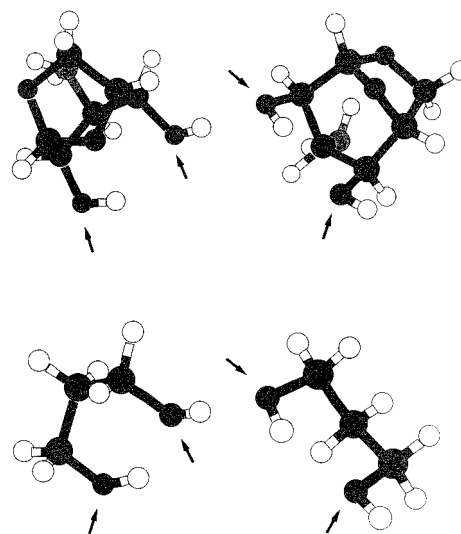
The values computed for complex I differ slightly from the experimental data measured for the dimer of the 1,3-diaxial diol sugar in chloroform solution,^{16b} which were found to be 3551 (O1-H1), 3331(O2-H2), 3593 (O3-H3) and 3685 (O4-H4) cm^{-1} , and for the hydrogen-bonded dimer of 1,4-butanediol in chloroform,³⁷ which were reported to be 3445 (O1-H1), 3270 (O2-H2), 3355 (O3-H3), and 3626 (O4-H4) cm^{-1} . Such differences are not surprising keeping in mind the simplicity of the model, the neglect of anharmonicity effects, and the lack of the solvent influence.³⁸ More importantly, the theoretical values for complex I reproduce quite well the ordering of experimental stretching frequencies for the different O-H groups. The results in Table 8 clearly show the red shift of the stretching frequencies of the donor and acceptor O-H groups in the central hydrogen bond on going from complex IV to complex I. Nevertheless, the frequencies of the terminal O-H groups (O1-H1; O4-H4) are little affected. According to the values for complexes I and IV, the frequency shift of the intermolecular hydrogen bond in complex I; $\nu(\text{free O-H}) - \nu(\text{O2-H2}) \approx 3677 - 3563 = 114$, is 78% larger than the shift observed for complex IV: $\nu(\text{free O-H}) - \nu(\text{O2-H2}) \approx 3677 - 3613 = 64$. This clearly indicates the relevant influence of cooperativity in hydrogen-bonded complexes.

The sensitivity of hydrogen-bond energetics to the immediate surroundings makes it necessary to examine the effect of neighboring functional groups in the sugar on the self-assembly. On this ground, the binding energy and relevant structural and electronic properties of the central hydrogen bond formed upon dimerization of the 1,3-diaxial diol pyranose ring were deter-

TABLE 8: Selected Properties Determined for the Dimers of 1,3-Diaxial Diol Pyranose Sugar and 1,3-Propanediol Dimers (Complex I)

property ^a	1,3-propanediol	pyranose sugar	
binding energy (kcal/mol) ^a	-6.7	-6.1	
bond distances (Å)	O2...O3	2.8624	2.8844
	O2-H2	0.9541	0.9533
	O3-H3	0.9508	0.9523
atomic charges (au)	O2	-0.821	-0.828
	H2	0.514	0.512
	O3	-0.792	-0.803
	H3	0.490	0.489
	H2...O3	0.0276	0.0256
electron density (au)	O2-H2	0.3540	0.3568
	O3-H3	0.3599	0.3581
	O1-H1	3636	3630
stretching frequencies (cm^{-1})	O2-H2	3563	3578
	O3-H3	3632	3617
	O4-H4	3677	3662

^a Values corrected corrected for the basis-set superposition error.

**Figure 3.** Optimized geometries for the dimer formed by two units of the model compound 1,3-propanediol and by the pyranose ring. The oxygens are marked by arrows.

mined. The optimized geometry of the dimer is shown in Figure 3, which shows a similar arrangement of the hydroxyl groups in the complex formed by the sugar rings and by the model compound.

The values of selected properties are given in Table 8, which also shows the corresponding results determined for the dimer of 1,3-propanediol for comparison purposes. There is close agreement between the two sets of values, which supports the preceding discussion about cooperativity effects. However, there are some significant differences. The binding energy for the sugar dimer is slightly lower than for the model compound, which agrees with the larger O2...O3 separation, the lower electron density at the bond critical point, and the larger stretching frequency in the pyranose dimer. However, the reduced binding energy does not fit with the larger charge separation in the hydroxyl groups, specially O3-H3, and the larger O3-H3 bond length in the pyranose dimer.

These peculiar features can be attributed to the presence of the endocyclic oxygen, which interact with the hydroxyl groups O1-H1 and O3-H3. This makes the endocyclic oxygen to be asymmetrically placed with respect to the two hydroxyl oxygens in each monomer, it being closer to O1 (O3) than to O2 (O4) by 0.01 (0.005) Å. These interactions weaken the intramolecular

hydrogen bonds O1—H1...O2 and O3—H3...O4, whose bond length is around 0.2 Å larger than that found for the dimer of 1,3-propanediol. Indeed, they also deviate from linearity around 7° more than in the dimer formed by the model compound. As a result, the cooperativity effect decreases, leading to a lower binding energy. Nevertheless, the interaction between the endocyclic oxygen and the group O3—H3 explains the enhanced charge separation of this hydroxyl group and the diminished electron density at its bond critical point, compared to the values obtained for the dimer of 1,3-propanediol.

The preceding discussion emphasizes the relevant role played by neighboring functional groups in modulating the cooperativity between hydrogen bonds. At this point, it is worth mentioning that the intrinsic free energy of intramolecular hydroxyl-to-ether oxygen hydrogen bond in hydroxy ethers can amount to -2.4 kcal/mol in low polar solvents.^{38a} This contribution is by no means negligible and points out that the hydroxyl-to-ether hydrogen bond can compete with the hydroxyl-to-hydroxyl one in the pyranose sugars considered in this study, thus interfering effectively the cooperative effect of intramolecular hydrogen bonds on the intermolecular hydrogen bonding.

The high content of hydroxyl groups in carbohydrates facilitates the formation of a dense network of hydrogen bonds. Of course, the strength of these interactions depends on factors modulating the optimal geometry between hydroxyl groups for hydrogen bonding, like the pattern of substitution of hydroxyl groups and their relative stereochemistry. Since electrostatics determines the value of the binding energy, achievement of a proper orientation between intra- and intermolecular hydrogen bonds is key for stabilizing the interactions in carbohydrates (see Table 2). Indeed, there are evidence supporting that the loss in entropy upon formation of intramolecular hydrogen bonds is lower than had been recognized,^{38a} probably due to the introduction of low-frequency vibrational modes. In this case, cooperativity effects are expected to contribute significantly to the binding energy, as noted in the enhancement of around 40% in the dimerization energy of complex I compared to complex IV (Table 1), and in the lowering of around 80% in the O—H vibrational frequency of the intermolecular hydrogen bond upon formation of two intramolecular hydrogen bonds (see above). In fact, our results suggests that cooperativity is crucial for the dimerization of this 1,6-anhydro-β-D-glucopyranoside derivative, which dimerizes in an open structure in the case of 1,3-diaxial diol derivatives, whereas self-assembly is not observed for the monoalcohol monomers.^{16b}

An interesting finding of the results discussed above is the role of potential donor/acceptor functional groups in the carbohydrates other than O—H on the formation of hydrogen-bonded networks. Particularly, the results show that the endocyclic oxygen plays an active role interfering the formation of the intramolecular hydrogen bond in the monomer. Similarly, the ether oxygen can also enhance the polarity of hydroxyl groups involved in hydrogen bonding, as noted in the case of the hydroxyl group O3—H3. Whether the effect of all these interactions enhances or diminishes the cooperativity effect between inter and intramolecular hydrogen-bonding depends on different factors, like the nature of the interacting functional groups and their geometrical arrangement. The implications of neighboring functional groups in the sugar on molecular recognition of carbohydrates cannot be neglected a priori. Rather, they can be viewed as structural elements susceptibles to be altered in order to modify the cooperativity and selectivity of hydrogen-bonded host—guest complexes.

Acknowledgment. This work was supported by the Centre de Supercomputació de Catalunya (CESCA; Molecular Recognition Project) and by the Dirección General de Investigación Científica y Técnica (DGICYT; Grants PB96-1005 and PB96-0833). M.L.P. thanks Comunidad de Madrid for a predoctoral fellowship.

References and Notes

- (1) Jeffrey, G. A.; Saenger, W. *Hydrogen Bonding in Biological Structures*; Springer: Berlin, 1991.
- (2) Lee, Y. C.; Lee, R. T. *Acc. Chem. Res.* **1995**, *28*, 321.
- (3) Kikuchi, Y.; Tanaka, Y.; Sutarto, S.; Kobayashi, K.; Toi, H.; Aoyama, Y. *J. Am. Chem. Soc.* **1992**, *114*, 10302.
- (4) Bourne, Y.; van Tilbeurgh, H.; Cambillau, C. *Curr. Opin. Struct. Biol.* **1993**, *3*, 681.
- (5) Bertozzi, C. R. *Chem. Biol.* **1995**, *2*, 703.
- (6) Frank, H. S.; Wen, W. Y. *Discuss. Faraday Soc.* **1957**, *24*, 133.
- (7) (a) Suhai, S. *J. Chem. Phys.* **1994**, *101*, 9766. (b) Ojamäe, L.; Hermansson, K. *J. Phys. Chem.* **1994**, *98*, 4271. (c) Contador, J. C.; Aguilar, M. A.; Sánchez, M. L.; Olivares del Valle, F. J. *J. Mol. Struct.: THEOCHEM* **1994**, *314*, 229. (d) Estrin, D. A.; Paglieri, L.; Corongiu, G.; Clementi, E. *J. Phys. Chem.* **1996**, *100*, 8701. (e) González, L.; Mó, O.; Yáñez, M.; Elguero, J. *J. Mol. Struct.: THEOCHEM* **1996**, *371*, 1. (f) Chen, W.; Gordon, M. J. *J. Phys. Chem.* **1996**, *100*, 14136. (g) Gresh, N. *J. Phys. Chem. A* **1997**, *101*, 8680. (h) Cruzan, J. D.; Braly, L. B.; Liu, K.; Brown, M. G.; Loeser, J. G.; Saykally, R. J. *Science* **1996**, *271*, 59. (i) Liu, K.; Brown, M. G.; Cruzan, J. D.; Saykally, R. J. *Science* **1996**, *271*, 62.
- (8) (a) Kelterbraun, R.; Turki, N.; Rahmouni, A.; Kochanski, E. *J. Mol. Struct.: THEOCHEM* **1994**, *314*, 191. (b) *Ibid. J. Chem. Phys.* **1994**, *100*, 1589.
- (9) (a) Zeegers-Huyskens, Th. *J. Mol. Struct.* **1993**, *297*, 149. (b) Karpfen, A.; Yanovitskii, O. *J. Mol. Struct.: THEOCHEM* **1994**, *314*, 211. (c) Liedl, K. R.; Kroemer, R. T.; Rode, B. M. *Chem. Phys. Lett.* **1995**, *246*, 455. (d) Packer, M. J.; Clary, D. C. *J. Phys. Chem.* **1995**, *99*, 14323. (e) Sear, R. P.; Jackson, G. *J. Chem. Phys.* **1996**, *105*, 1113. (f) Tschumper, G. S.; Yamaguchi, Y.; Schaefer, H. F. *J. Chem. Phys.* **1997**, *106*, 9627.
- (10) (a) Suhai, S. *Int. J. Quantum Chem.* **1994**, *52*, 395. (b) King, B. F.; Weinhold, F. *J. Chem. Phys.* **1995**, *103*, 333. (c) King, B. F.; Farrar, T. C.; Weinhold, F. *J. Chem. Phys.* **1995**, *103*, 348. (d) Karpfen, A. *J. Phys. Chem.* **1996**, *100*, 13474.
- (11) Mó, O.; Yáñez, M.; Rozas, I.; Elguero, J. *J. Chem. Phys.* **1994**, *100*, 2871.
- (12) Peeters, D.; Leroy, G. *J. Mol. Struct.: THEOCHEM* **1994**, *314*, 39. (b) Mó, O.; Yáñez, M.; Elguero, J. *J. Mol. Struct.: THEOCHEM* **1994**, *314*, 73.
- (13) (a) Shivaglal, M. C.; Singh, S. *Int. J. Quantum Chem.* **1992**, *44*, 679. (b) Privalov, P. L.; Makhatadze, G. I. *J. Mol. Biol.* **1993**, *232*, 660. (c) Schäfer, L.; Newton, S. Q.; Cao, M.; Peeters, A.; Van Alsenoy, C.; Wolinski, K.; Momany, F. A. *J. Am. Chem. Soc.* **1993**, *115*, 272. (d) Guo, H.; Karplus, M. *J. Phys. Chem.* **1994**, *98*, 7104. (e) Gung, B. W.; Zhu, Z. *Tetrahedron Lett.* **1996**, *37*, 2189.
- (14) (a) Craig, B. N.; Janssen, M. U.; Wickersham, B. M.; Rabb, D. M.; Chang, P. S.; O'Leary, D. *J. Org. Chem.* **1996**, *61*, 9610. (b) Pearce, C. M.; Sanders, J. K. M. *J. Chem. Soc., Perkin Trans 1* **1994**, 1119. (c) Uhlman, P.; Vasella, A. *Helv. Chim. Acta* **1992**, *75*, 1979. (d) Muddasani, P. R.; Bernet, B.; Vasella, A. *Helv. Chim. Acta* **1994**, *77*, 334. (e) Notelmeyer, M.; Saenger, W. *J. Am. Chem. Soc.* **1980**, *102*, 2710. (f) Vyas, N. K.; Vyas, M. N.; Quiocho, F. A. *Science* **1988**, *242*, 1290. (g) Vyas, N. K. *Curr. Opin. Struct. Biol.* **1991**, *1*, 732.
- (15) (a) Zhbakov, R. G. *J. Mol. Struct.* **1992**, *270*, 523. (b) Jorgensen, W. L.; Damm, W.; Frontera, A.; Lamb, M. L. In *Physical Supramolecular Chemistry*; Echegoyen, L.; Kaifer, A. E., Eds.; Kluwer: Amsterdam, 1996; pp 115–126.
- (16) (a) López de la Paz, M.; Ellis, G.; Penadés, S.; Vicent, C. *Tetrahedron Lett.* **1997**, *38*, 1659. (b) López de la Paz, M.; Jiménez-Barbero, J.; Vicent, C. *Chem. Commun.* **1998**, 465.
- (17) Hariharan, P. C.; Pople, J. A. *Theor. Chim. Acta* **1973**, *28*, 213.
- (18) (a) McLean, A. D.; Chandler, G. S. *J. Chem. Phys.* **1980**, *72*, 5639. (b) Frisch, M. J.; Pople, J. A.; Binkley, J. S. *J. Chem. Phys.* **1984**, *80*, 3265. (c) Clark, T.; Chandrasekhar, J.; Spitznagel, G. W.; Schleyer, P. v. R. *J. Comput. Chem.* **1983**, *4*, 294.
- (19) Möller, C.; Plesset, M. S. *Phys. Rev.* **1934**, *46*, 618.
- (20) (a) Becke, A. D. *J. Chem. Phys.* **1993**, *98*, 5648. (b) *Ibid.* **1988**, *88*, 1053. (c) Lee, C.; Yang, W.; Parr, R. G. *Phys. Rev. B* **1988**, *37*, 785.
- (21) Pople, J. A.; Head-Gordon, M.; Fox, D. J.; Raghavachari, K.; Curtiss, L. A. *J. Chem. Phys.* **1989**, *90*, 5622.
- (22) Boys, S. F.; Bernardi, F. *Mol. Phys.* **1970**, *19*, 553.
- (23) (a) Luque, F. J.; Orozco, M. *J. Comput. Chem.* **1998**, *19*, 866. (b) Cubero, E.; Luque, F. J.; Orozco, M. *Proc. Natl. Acad. Sci. U.S.A.* **1998**, *95*, 5976. (c) Molecular Electrostatic Potentials: Concepts and Application.

In *Theoretical and Computational Chemistry*; Murray, J. S., Sen, K., Eds.; Elsevier: Amsterdam, 1996; Vol. 3, pp 181–178.

- (24) Scrocco, E.; Tomasi, J. *Top. Curr. Chem.* **1973**, *42*, 95.
(25) Francl, M. M. *J. Phys. Chem.* **1985**, *89*, 428.
(26) (a) Momany, F. A. *J. Phys. Chem.* **1978**, *85*, 592. (b) Besler, B. H.; Merz, K. M., Jr.; Kollman, P. J. *Comput. Chem.* **1990**, *11*, 431. (c) Orozco, M.; Luque, F. J. *J. Comput. Chem.* **1990**, *11*, 909.
(27) Alhambra, C.; Luque, F. J.; Orozco, M. *J. Phys. Chem.* **1995**, *99*, 3084.
(28) (a) Bader, R. F. W. *Atoms in Molecules. A Quantum Theory*; Clarendon: Oxford, 1990. (b) Bader, R. F. W. *Chem. Rev.* **1991**, *91*, 893. (c) Bader, R. F. W.; Carroll, M. T.; Cheeseman, J. R.; Chang, C. *J. Am. Chem. Soc.* **1987**, *109*, 7968.
(29) Frisch, M. J.; Trucks, G. W.; Schlegel, H. B.; Gill, P. M. W.; Johnson, B. G.; Robb, M. A.; Cheeseman, J. R.; Keith, T. A.; Petersson, G. A.; Montgomery, J. A.; Raghavachari, K.; Al-Laham, M. A.; Zakrzewski, V. G.; Ortiz, J. V.; Foresman, J. B.; Cioslowski, J.; Stefanov, B. B.; Nanayakkara, A.; Challacombe, M.; Peng, C. Y.; Ayala, P. Y.; Chen, W.; Wong, M. W.; Anfrues, J. L.; Replogle, E. S.; Gomperts, R.; Martin, R. L.; Fox, D. J.; Binkley, J. S.; Defress, D. J.; Baker, J.; Stewart, J. J. P.; Head-Gordon, M.; Gonzalez, C.; Pople, J. A. *GAUSSIAN 94* (Rev. A.1); GAUSSIAN Inc.: Pittsburgh, PA, 1995.
(30) Biegler-König, F.; Bader, R. F. W.; Tang, T.-H. *J. Comput. Chem.* **1982**, *3*, 317.

(31) Luque, F. J.; Orozco, M. Unpublished version of MOPETE/MOPFIT computer programs, University of Barcelona: Barcelona, Spain.

- (32) (a) Bizzari, A.; Stolte, S.; Reuss, J.; van Duijneveldt-van de Rijdt, J. G. C. M.; van Duijneveldt, F. B. *Chem. Phys.* **1990**, *143*, 423. (b) Zheng, Y. J.; Merz, K. M. *J. Comput. Chem.* **1992**, *13*, 1152. (c) Colomines, C.; Teixidó, J.; Cemeli, J.; Luque, F. J.; Orozco, M. *J. Phys. Chem.*, in press.
(33) Mulliken, R. S. *J. Chem. Phys.* **1955**, *23*, 1833.
(34) (a) Boyd, R.; Choi, S.; Cheng. *Chem. Phys. Lett.* **1985**, *120*, 80. (b) *Ibid.* **1986**, *129*, 62. (c) Carroll, M. T.; Bader, R. F. W. *Mol. Phys.* **1988**, *65*, 695. (d) Tang, T. H.; Hu, W. J.; Yan, D. Y.; Cui, Y. P. *J. Mol. Struct.: THEOCHEM* **1990**, *207*, 319. (e) Koch, U.; Popelier, P. L. A. *J. Phys. Chem.* **1995**, *99*, 9747.
(35) (a) Gatti, C.; MacDougall, P. J.; Bader, R. F. W. *J. Chem. Phys.* **1988**, *88*, 3792. (b) Boyd, R. J.; Wang, L. C. *J. Comput. Chem.* **1989**, *10*, 367.
(36) (a) Huyskens, P. L. *J. Am. Chem. Soc.* **1977**, *99*, 2578. (b) Kleeberg, H.; Heinje, G.; Luck, W. A. P. *J. Phys. Chem.* **1986**, *90*, 4427. (c) Maes, G.; Smets, J. *J. Phys. Chem.* **1993**, *97*, 1818.
(37) Kleeberg, H.; Klein, D.; Luck, W. A. P. *J. Phys. Chem.* **1987**, *91*, 3200.
(38) (a) Beeson, C.; Pham, N.; Shipps, G., Jr.; Dix, T. A. *J. Am. Chem. Soc.* **1993**, *115*, 6803. (b) Luck, W. A. P.; Klein, D. *J. Mol. Struct.* **1996**, *381*, 83.